Title

Framework to Enable Regional 3D Probabilistic Assessment of Excavation Induced Structural Damage Using a Monte-Carlo Method

Journal

GEO-RISK 2023: DEVELOPMENTS IN RELIABILITY, RISK, AND RESILIENCE, 346(GSP 346)

ISSN

0895-0563

Authors

Zhao, Jinyan
Ritter, Stefan
DeJong, Matthew J

Publication Date

2023-07-20

DOI

10.1061/9780784484982.004

Framework to Enable Regional 3D Probabilistic Assessment of Excavation Induced Structural Damage Using a Monte-Carlo Method

Jinyan Zhao, Ph.D. Student,[1] Stefan Ritter, Ph.D.,[2] and Matthew J. DeJong, Ph.D.[3]

[1,3]Structural Engineering, Mechanics and Materials, Department of Civil and Environmental Engineering, University of California, Berkeley, CA, USA, 94720; E-mail: jinyan_zhao@berkeley.edu, dejong@berkeley.edu

[2]Onshore foundation section, Norwegian Geotechnical Institute, Oslo, Norway, P.O. Box. 3930, E-mail: stefan.ritter@ngi.no

ABSTRACT

This paper presents a framework to enable probabilistic assessment for braced excavation-induced structural damage on a regional scale. Random filed models are created to describe the uncertainties of spatially variable ground displacements induced by excavation, and random variables are adopted to model the uncertainties of soil stiffnesses, structural stiffnesses, and building weights. The uncertainties are propagated to the probability distributions of building characteristic tensile strains (ε_c) through a Monte-Carlo method, in which a 3-dimensional (3D) soil-structure interaction (SSI) model is evaluated in each simulation. With limit state functions defined based on ε_c, damage probabilities were quantified for all buildings in the region impacted by the excavation. Fragility heatmaps that can be used for estimating the probabilities of each possible damage state from impact level were also generated for each building. The framework is demonstrated with an excavation case history executed in Oslo, Norway. The 3D SSI model adopted in the framework can provide more accurate building response prediction than conventional 2D analysis. Meanwhile, the probabilistic assessment method provides a tool to quantify the uncertainty effect in the building assessment of large excavation construction.

1. INTRODUCTION

Braced excavations are commonly executed in urban areas, where many buildings might be impacted by excavation-induced ground displacements. Such ground displacements may cause severe damages to adjacent buildings (e.g., Bryson and Kotheimer 2011 and Korff et al. 2011), and it is essential to quantify the potential structural damages when the excavations are designed and executed. Soil-structure interaction (SSI) models with different levels of fidelity (e.g., Finno et al. 2005, Son and Cording 2005, and Dong et al. 2022) have been proposed to estimate such structural damages. However, the low-fidelity SSI models, such as the methods based on equivalent beams and modification factors, may suffer from large uncertainty (e.g., Zhao et al. 2022). Furthermore, the knowledge required and the certainty in input data to calibrate high-fidelity SSI models are usually not available in most design and construction scenarios, which prohibits the usage of such high-fidelity models in practice. Moreover, the modeling efforts of high-fidelity models are generally not affordable for regional scale assessment, where a large number of buildings need to be analyzed. The 3-dimensional (3D) 2-stage SSI model first proposed in Zhao and DeJong (2022) is

believed to achieve an accurate building response prediction with a reasonable modeling complexity and is adopted in this paper to realize a regional scale assessment. The 3D SSI model was originally proposed for tunneling-induced building damage quantification. The 3D SSI model presented in this paper can provide a more accurate prediction of building response to deep excavation than conventional 2D models that are most commonly adopted in current engineering practice. Moreover, the probabilistic framework enables a rigorous quantification of the uncertainty in the performance assessment of building response to deep excavations, while the modeling and computation effort remains reasonable so that regional assessment can be achieved.

This paper introduces the extension of this 3D SSI model to braced excavations, which is described in section 2. The extended 3D SSI model may experience uncertainties caused by ground displacement prediction and modeling parameters, and probabilistic methods are usually adopted to facilitate decision-making under uncertainties. In section 3, a Monte-Carlo based regional probabilistic assessment framework is proposed, in which a spatial variable regional ground displacement model is developed, and the uncertainty modeling methods for soil and structural properties are suggested. Section 4 describes the application of the proposed probabilistic assessment framework in an excavation case history in Oslo, Norway, and some conclusions are presented in the final section.

2. 3-DIMENSIONAL (3D) 2-STAGE SSI MODEL FOR BRACED EXCAVATION

Zhao and DeJong (2022) developed a 3D 2-stage SSI model based on the 2-dimensional soil-structure interface model first proposed by Franza and DeJong (2019). In the 2-stage approach, ground displacements are first estimated and applied as displacement boundary conditions on the soil-structure interface. In this paper, the vertical and horizontal ground displacements induced by braced excavations are estimated from a smoothed version (Eq. 1) of the KJHH & KSJH model (Kung et al. 2007 and Schuster 2009), where dv is the vertical displacement, dl is the lateral displacement, H is the excavation depth, x is the distance to excavation wall, and η is a parameter describing the width of the settlement trough. The estimated ground displacements are then applied on an elastoplastic soil-structure interface illustrated in Fig. 1(b). The soils are modeled as a semi-infinite elastic continuum, and the soil stiffness coefficients at each soil-structure interface node can be calculated with Mindlin's solutions. In the vertical direction, the surface structures are connected to the soil through rigid plastic sliders with zero tensile strength to simulate the formation of gaps between buildings and soil. In the horizontal direction, sliders with strength equal to the vertical compressive stress multiplied by a friction coefficient are implemented to simulate Coulomb's friction model at the interface. The surface buildings are modeled with the finite element method (FEM), and the deformation of the buildings can be solved with typical FEM theories. The formulation of the whole SSI system can be found in Zhao and DeJong (2022), and such an elastoplastic interface model is an effective way to solve the small displacement and non-penetration problems in contact mechanics.

Fig 2. presents the SSI models created for two buildings in the case study area. The FEM meshes and calculated ε_c (which is defined as the 99% quantile of the principal tensile strains in all building elements as suggested in Yiu et al. 2017) are shown in Fig. 2(c-d). Fig. 3 is a comparison of the monitored vertical displacement at the building corners with the values calculated with the proposed SSI model using the greenfield ground displacements approximated from the field

monitoring data after the excavation is completed. Because only one cross-section can be estimated from the monitored settlements, the ground settlement profile under the region was assumed to be the same along the excavation wall. However, as discussed in Section 3, the ground settlement profile may show spatial variability along the excavation boundary. Considering the large uncertainty caused by the estimated greenfield ground displacements, Fig. 3 suggests that an accurate building response can be obtained from the proposed SSI model if accurate greenfield ground displacements are known. However, it should be noted that such greenfield ground displacements can only be approximated after the construction is completed, and they are usually influenced by additional consolidation settlement induced by porewater pressure reduction caused by construction activities. In early design stages, the greenfield displacement profiles are usually estimated from experience obtained in engineering practice and may suffer large uncertainty. A spatial variable model described later is suggested to model such uncertainty in the predicted greenfield ground displacements.

$$\frac{dv\left(\frac{x}{H}\right)}{H} = \frac{dv_{max}}{H}\frac{1.14}{\frac{x/H}{\eta}+0.39}\frac{1}{0.46\sqrt{2\pi}}\exp\left(-\frac{\left(ln\left(\frac{x/H}{\eta}+0.39\right)-0.095\right)^2}{0.423}\right)$$
$$\frac{dl\left(\frac{x}{H}\right)}{H} = \frac{dl_{max}}{H}\frac{2.14}{\frac{x/H}{\eta}+0.82}\frac{1}{0.44\sqrt{2\pi}}\exp\left(-\frac{\left(ln\left(\frac{x/H}{\eta}+0.82\right)-0.80\right)^2}{0.387}\right) \quad (1)$$

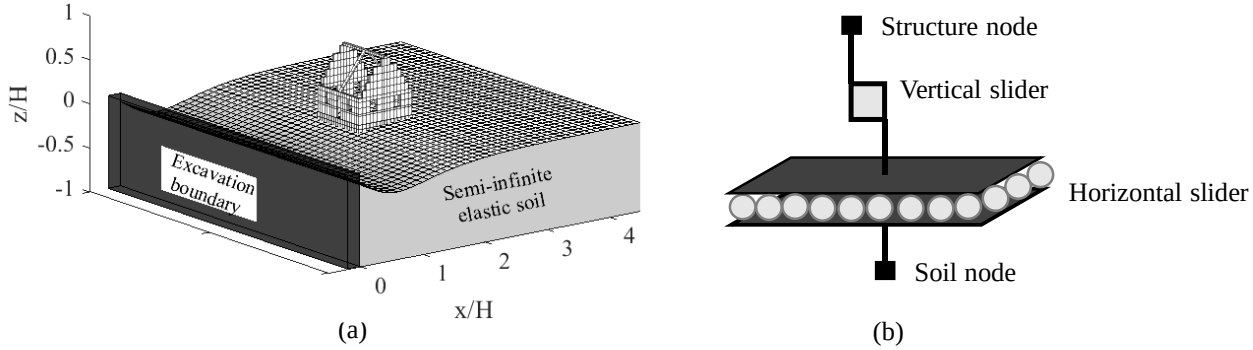

Fig. 1 (a) Schematic 3D SSI model (b) 3D elastoplastic soil-structure interface model

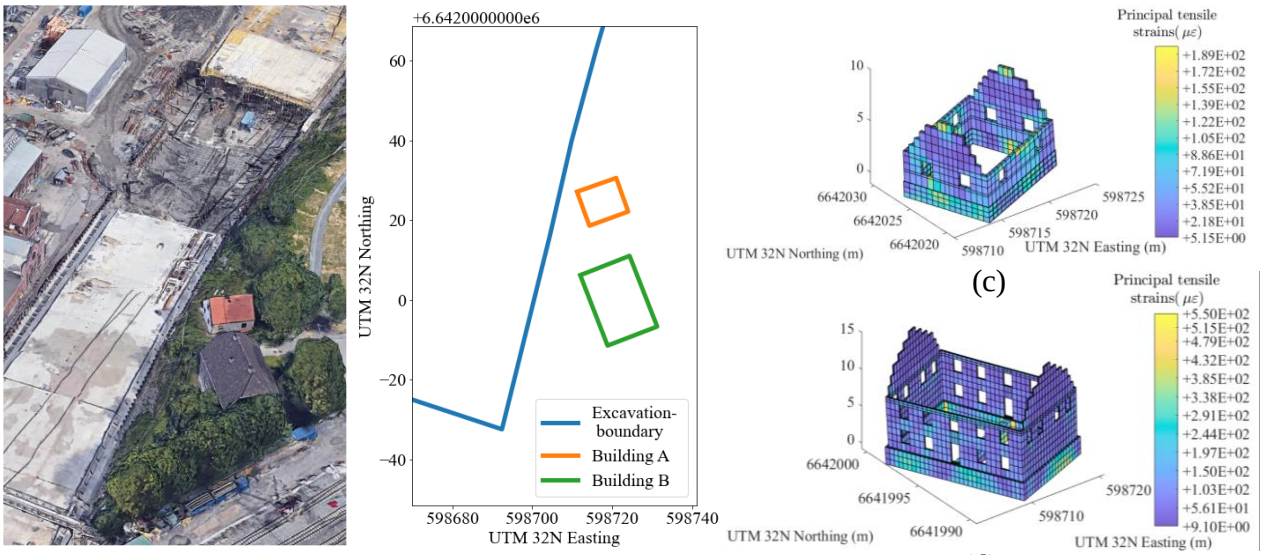

Fig. 2 (a) Bird's eye view of the case study area (from Google Earth); (b) Location of the excavation wall and studied buildings; (c) 3D SSI model of building A and distribution of principal tensile strains; (d) 3D SSI model of building B and distribution of principal tensile strains.

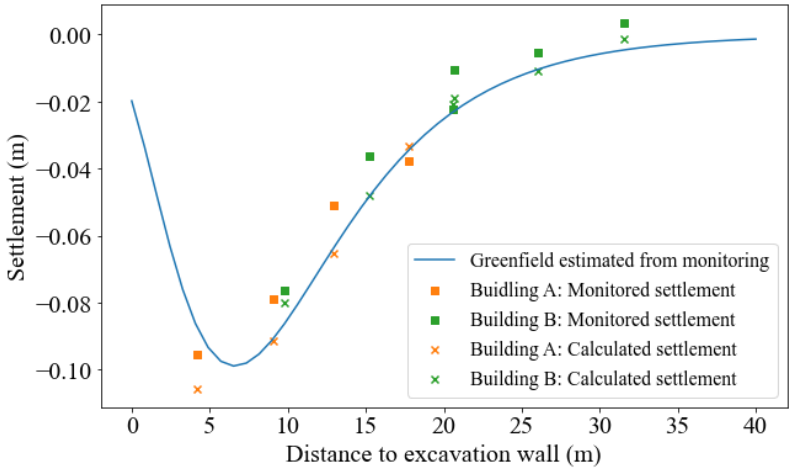

Fig. 3 Comparison of monitored and calculated building settlements.

3. UNCERTAINTY MODELING AND PROPAGATION METHOD

A large number of excavation-induced ground displacement records in Norway were collected in Langford et al. (2016). Although Eq. 1 can generally provide a reasonable prediction for ground displacement profiles, the data of the collected case histories indicate that the maximum ground displacement (dv_{max}/H) and width of the profile (η) show large variances. A study of the greenfield ground displacement records in the Oslo area also suggests that these two variables at different cross-sections are spatially correlated, depending on the distance between the cross-sections, and dv_{max}/H and η are statistically independent from each other. As a result, the spatial correlation is estimated from the ground displacement records and used to model the spatial variability of the predicted ground displacements. To ensure dv_{max}/H and η are positive-definite in the uncertainty models, empirical variograms are estimated in the logarithmic space (i.e., $log(dv_{max}/H)$

and $log(\eta)$). Fig. 4 shows the empirical Cressie's semivariance and the Gaussian variogram models created for $log(dv_{max}/H)$ and $log(\eta)$. Further assuming normal marginal distributions for $log(dv_{max}/H)$ and $log(\eta)$, lognormal random field models that capture the ground spatial variable behavior in the Oslo area are obtained for dv_{max}/H and η. It is noteworthy that the empirical semivariance with long lags (i.e., points to the right of Fig. 4(a) and Fig. 4(b)) are estimated with a small amount of data and may experience large biases. The empirical semivariance and corresponding variogram models can be refined with our framework when more greenfield ground displacement monitoring records become available.

With the random field models defined for dv_{max}/H and η, samples of the ground displacements at each surface structure node can be generated with discrete Karhunen-Loève expansion (Schenk and Schuëller 2005) and fed to the Monte-Carlo based uncertainty propagation framework proposed in Zhao et al. (2022). Uncertainties in the estimation of soil stiffness (E_s), building stiffness (E_b) and building loads (L) are also considered in this paper, and their uncertainty models are suggested in a variety of literature (e.g., Ellingwood 1980, Lacasse and Nadim 1997, and Phoon and Kulhawy 1999). The computer program UQESI developed by Zhao et al. (2022) is extended to incorporate the 3D SSI model and then adopted for propagating the uncertainties from input parameters to ε_c in each of the surface buildings in the impacted region. The extended UQESI can run in both personal computers and high-performance computer clusters, and its output is the empirical probability density function of ε_c in each building. The damage probabilities of each building can then be estimated according to the widely used limit states defined in Boscardin and Cording (1989), and fragility heatmaps can be developed by estimating the damage probabilities conditioned on different impact levels.

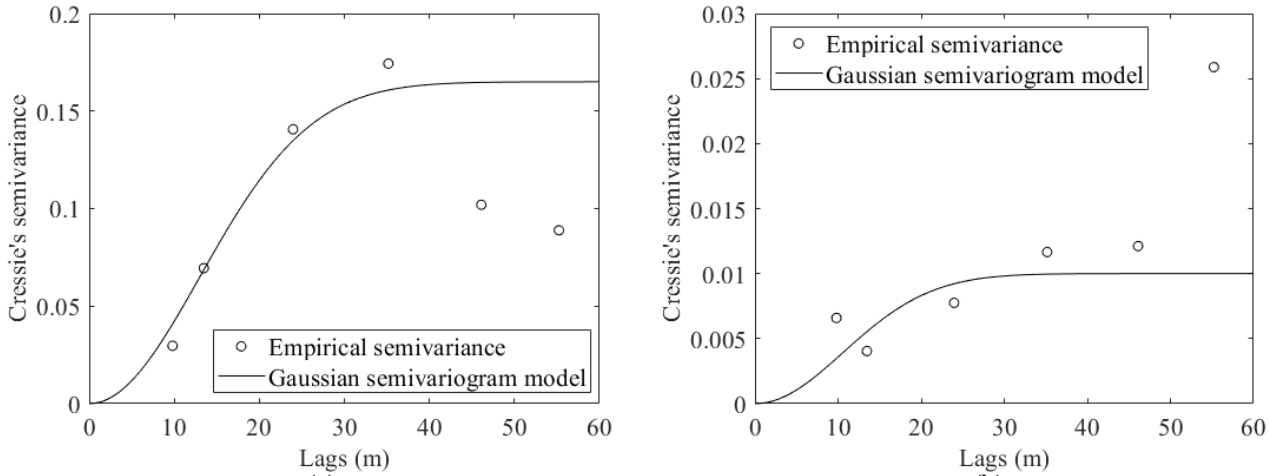

Fig. 4. Empirical semivariance and Gaussian semivariogram model for (a) $log(dv_{max}/H)$, and (b) $log(\eta)$.

4. CASE STUDY

A segment of an infrastructure project in Oslo is presented to demonstrate the proposed regional probabilistic assessment framework. The excavation depth is about 11 m deep and supported by steel props and concrete slabs. Sheet piles were first piled until the bedrock level, and the top concrete slab and steel props were then installed. Afterward, internal excavation was carried on, after which the bottom slab and internal

vertical concrete walls were cast. The excavated soil was mostly clay, with an initial elastic modulus of approximately 50 MPa. To account for the stiffness reduction caused by very large soil strain induced by the excavation, a $(17.9 \times beta(2,2) + 1.06) \times 10^6$ distribution, which corresponds to a 10 MPa mean and 40% coefficient of variance (CoV), is used to model the uncertainty of the soil elastic modulus used in the SSI model. The 40% CoV is consistent with the suggestions given in Phoon and Kulhawy (1999).

Only two buildings (Building A and B in Fig. 2) are in the vicinity of the studied excavation segment and are analyzed here. However, the same approach can be readily applied to the buildings in the whole region impacted by the excavation, and a regional probabilistic assessment can be achieved. The Matlab package MasonMesh (Zhao (2023)) can be adopted for fast FEM mesh generation if a large number of buildings are analyzed. Building A consists of solid bricks and mortar, and the nominal stiffness of building A was estimated to be 1700 MPa, as suggested in the European Standard (2005). Building B is a timber building with hewn masonry foundations, and the nominal stiffness for timber and structure are respectively estimated as 1200 MPa and 1400 MPa. The buildings were built more than 200 years ago, and to account for the degradation, a reduction factor (RF) with the distribution $0.45 \times beta(2,4) + 0.55$ is applied to the building stiffness. This reduction factor is consistent with the strength reduction factor adopted in ASCE 5/ACI 530 (2011), which suggested a small probability (10% in the proposed distribution) that the RF is smaller than 0.6. $beta(2,4)$ is adopted for RF so that the distribution is skewed to the right, which ensures a conservative estimation of the building stiffness. To model the uncertainty in the estimation of building weight (L), the method suggested in Ellingwood (1980) is adopted, where the mean of L was taken as 1.05 of the nominal design loads and a CoV of 10% should be considered. The nominal design loads on the buildings were taken as the material self-weight plus 10 kPa per story, and a normal distribution is assumed for L. With the input uncertainty from ground displacement and modeling parameters quantified for the studied buildings, 1500 Monte-Carlo simulations were conducted for each building to estimate the distribution of their ε_c. The Monte-Carlo simulations were completed in the high-performance computer cluster SAVIO at UC Berkeley and the computation took around 15-20mins for each studied building.

Fig. 5(a) and Fig. 5(b) show the empirical cumulative density distribution of ε_c for building A and B respectively. The vertical lines are the limiting tensile strains for damage categories proposed in Boscardin and Cording (1989), which are commonly used in the damage classification of masonry buildings. Fig. 5(a) suggests that building A will most likely (84%) experience "Negligible" damage with a very small chance of experiencing some "Very Slight" damages. This is consistent with the observations made after the excavation, in which some hairline cracks (around 0.1 mm) were found at the window corners. Fig. 5(b) suggests that building B will most likely (55%) experience "Very Slight" damage, and there is around a 20% probability of experiencing "Slight" damage. Burland et al. (2004) suggest that a "Very Slight" damage stands for easily treated fine cracks with typical crack widths up to 1 mm and "Slight" damage stands for a damage state that re-decoration is required with typical crack widths up to 5 mm. Such descriptions are consistent with the damage observed in building B. However, the ground continued settling after the excavation due to consolidation, and the consolidation settlement has caused more damage than the short-term damage estimated in this paper. Consolidation effects could also be considered in this modeling framework but are not considered here.

Fig 6 and Fig 7 are the fragility heatmaps estimated from the Monte Carlo simulation results for building A and B. The horizontal axes are the maximum settlement of the corresponding building, and the vertical axes are the ε_c values that developed in the building. If a prediction is made for the impact level of a building (i.e., the predicted maximum settlement of a building falls in one of the vertical strips), the probabilities of each damage state for this building can be estimated by dividing the number of points in each damage state block by the total number of points in the vertical strip. As a result, when an impact level

is known, the total probability of all possible damage states is one. If curves (typically lognormal curves) are fitted for the damage probabilities in each horizontal strip, fragility curves describing the probability of each damage state at different building settlement levels can be approximated. During construction, updated building settlement predictions are usually made based on observed on-site conditions, and sometimes based on unexpected construction activities. The fragility heatmaps can be used to quickly update the damage probabilities according to the updated building settlement prediction without running the Monte-Carlo simulations again.

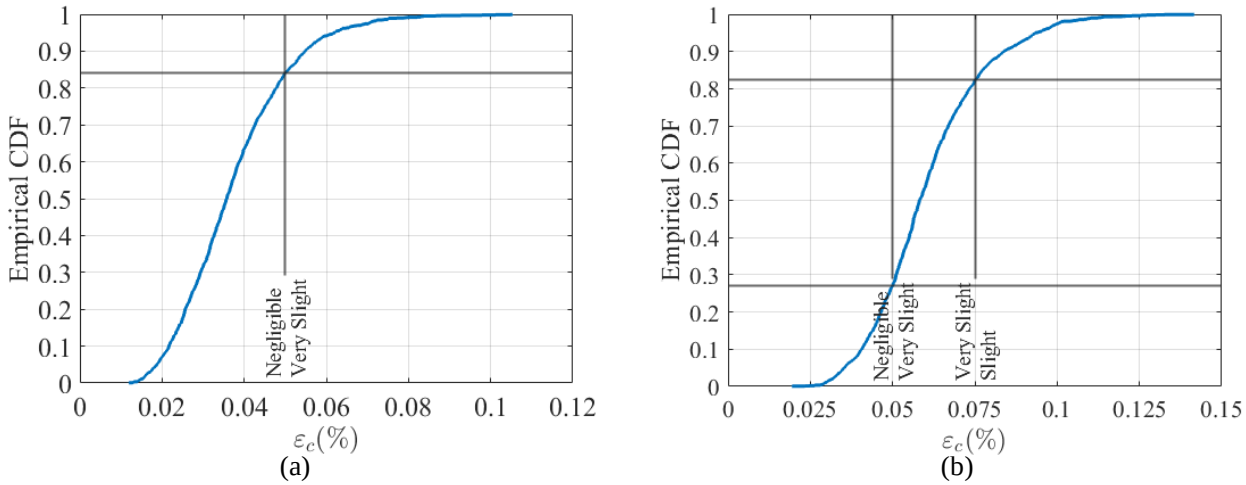

Fig. 5. Empirical cumulative density functions (CDFs) for (a) building A and (b) building B.

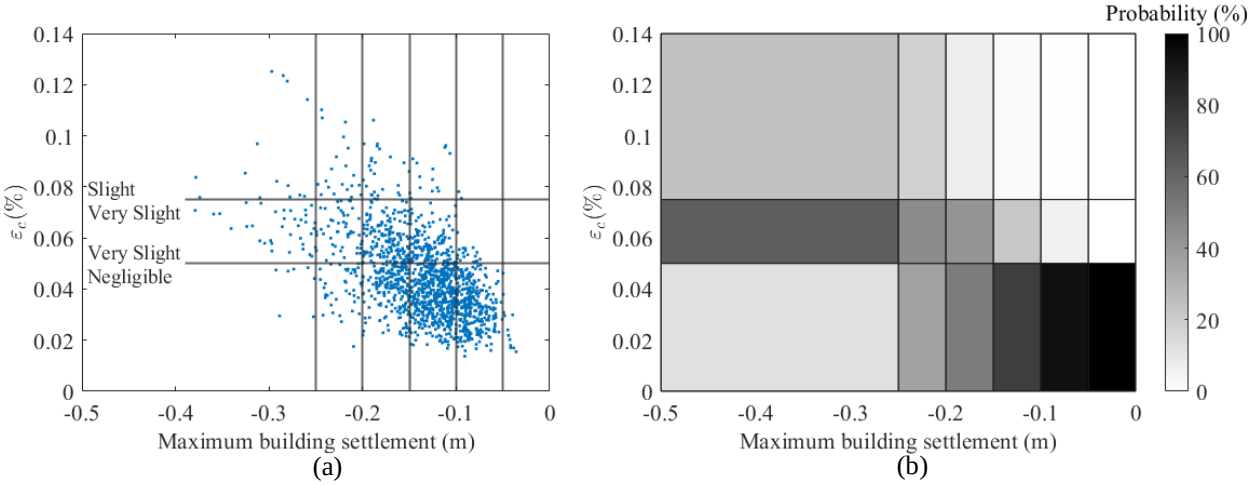

Fig. 6. (a) Scatter plot of ε_c versus maximum building settlement for building A and (b) Fragility heatmap for building A.

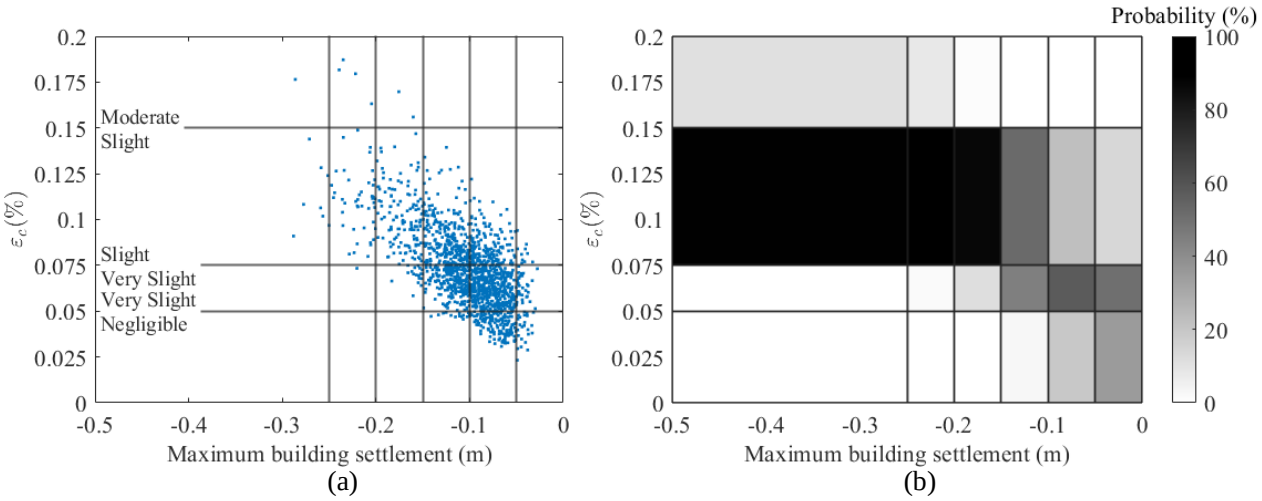

Fig. 7. (a) Scatter plot of ε_c versus maximum building settlement for building B and (b) Fragility heatmap for building B.

5. CONCLUSIONS

A framework that enables regional probabilistic assessment for braced excavation induced building damage is developed. 3D soil-structure interaction models were adopted to significantly reduce the uncertainty caused by the building shape and orientation to the excavation boundary compared to the state-of-the-practice using 2D equivalent beam methods. The spatial variable behavior for excavation induced greenfield ground displacement in Oslo area was estimated through case history data, and a spatial variable ground displacement model assuming Gaussian variogram models and lognormal random fields was proposed. The uncertainties of the ground displacements, soil stiffnesses, building stiffnesses, and building weights were quantified for a portion of an excavation project in Oslo and the capability of the proposed regional probabilistic assessment was demonstrated. The probabilistic assessment results for the studied buildings show a reasonable comparison with the observed damage. Fragility heatmaps were developed, which can be used as a tool for real-time updating of building damage probabilities using updated building settlements prediction made according to monitoring during the construction process.

6. ACKNOWLEDGEMENTS

The authors are grateful to the Peder Sather Centre for funding parts of this research. The authors would also like to thank the Norwegian National Rail Administration (Bane NOR) and the Restaurering AS for the information on the case study. The authors would also like to thank senior engineer Thomas Sandene and project engineer Luca Piciullo at the Norwegian Geotechnical Institute (NGI) for the kind discussion and advice

7. REFERENCES

ACI 530/ACI 5 (2011). Building Code Requirements and Specification for Masonry Structures. *Masonry Standards Joint Committee of the Masonry Society*.

Boscardin, M. D., & Cording, E. J. (1989). Building Response to Excavation-Induced Settlement. Journal of Geotechnical Engineering, 115(1), 1-21.

Bryson, L. S., & Kotheimer, M. J. (2011). Cracking in Walls of a Building Adjacent to a Deep Excavation. Journal of performance of constructed facilities, 25(6), 491-503.

Burland, J. B., Mair, R. J., & Standing, J. R. (2004). Ground Performance and Building Response Due to Tunnelling. In Advances in geotechnical engineering: The Skempton conference: Proceedings of a three day conference on advances in geotechnical engineering, organized by the Institution of Civil Engineers and held at the Royal Geographical Society, London, UK, on 29–31 March 2004 (pp. 291-342). Thomas Telford Publishing.

Dong, Y. P., Burd, H. J., & Houlsby, G. T. (2022). Finite-Element Investigation of Excavation-Induced Settlements of Buildings and Buried Pipelines. Journal of Geotechnical and Geoenvironmental Engineering, 148(10), 04022072.

Ellingwood, B. (1980). Development of A Probability Based Load Criterion for American National Standard A58: Building Code Requirements for Minimum Design Loads in Buildings and Other Structures (Vol. 577). Department of Commerce, National Bureau of Standards.

European Standard (2005) Eurocode 6 – Design of Masonry Structures Part 1-1: General rules for reinforced and unreinforced masonry structures.

Finno, R. J., Voss Jr, F. T., Rossow, E., & Blackburn, J. T. (2005). Evaluating damage Potential in Buildings Affected by Excavations. Journal of geotechnical and geoenvironmental engineering, 131(10), 1199-1210.

Franza, A., & DeJong, M. J. (2018). Elastoplastic Solutions to Predict Tunnelling-Induced Load Transfer and Deformation Mechanisms of Surface Structures. Journal of Geotechnical and Geoenvironmental Engineering.

Korff, M., Mair, R. J., Van Tol, A. F., & Kaalberg, F. (2011). Building damage and repair due to leakage in a deep excavation. Proceedings of the Institution of Civil Engineers-Forensic Engineering, 164(4), 165-177.

Kung, G. T., Juang, C. H., Hsiao, E. C., & Hashash, Y. M. (2007). Simplified model for wall deflection and ground-surface settlement caused by braced excavation in clays. Journal of Geotechnical and Geoenvironmental Engineering, 133(6), 731-747.

Lacasse, S., & Nadim, F. (1997). Uncertainties in characterising soil properties. Publikasjon-Norges Geotekniske Institutt, 201, 49-75.

Langford, J., Karlsrud, K., Lande, E. J., Baardvik, G., Engen, A. (2016). BegrensSkade – Limitation of damage caused by groundworks. In: Grundl¨aggningsdagen GD2016. Stock-holm, Sweden

Phoon, K. K., & Kulhawy, F. H. (1999). Characterization of geotechnical variability. Canadian geotechnical journal, 36(4), 612-624.

Schenk, C. A., & Schuëller, G. I. (2005). Uncertainty assessment of large finite element systems (Vol. 24). Springer Science & Business Media.

Schuster, M., Kung, G. T. C., Juang, C. H., & Hashash, Y. M. (2009). Simplified model for evaluating damage potential of buildings adjacent to a braced excavation. Journal of geotechnical and geoenvironmental engineering, 135(12), 1823-1835.

Son, M., & Cording, E. J. (2005). Estimation of building damage due to excavation-induced ground movements. Journal of geotechnical and geoenvironmental engineering, 131(2), 162-177.

Yiu, W. N., Burd, H. J., & Martin, C. M. (2017). Finite-Element Modelling for the Assessment of Tunnel-Induced Damage to a Masonry Building. Géotechnique, 67(9), 780-794.

Zhao, J., Ritter, S., & DeJong, M. J. (2022). Early-stage assessment of structural damage caused by braced excavations: Uncertainty quantification and a probabilistic analysis approach. Tunnelling and Underground Space Technology, 125, 104499.

Zhao, J., (2023). MasonMesh Matlab (https://www.mathworks.com/matlabcentral/fileexchange/123345-masonmesh). *MATLAB Central File Exchange.*

Zhao, J., & DeJong, M. J. (2023). Three-dimensional probabilistic assessment of tunneling induced structural damage using Monte-Carlo method and hybrid finite element model. Computers and Geotechnics, 154, 105122.